Journal of Materials Chemistry A

PAPER

View Article Online
View Journal | View Issue

Massive-exfoliation of magnetic graphene from acceptor-type GIC by long-chain alkyl amine†

Cite this: J. Mater. Chem. A, 2014, 2, 4244

Masaki Ujihara,*[a] Mahmoud Mohamed Mahmoud Ahmed,[a] Toyoko Imae*[ab] and Yusuke Yamauchi[c]

Graphene can be prepared from a graphite intercalation compound (GIC) with acceptor-type intercalator, $FeCl_3$. When the $FeCl_3$–GIC is treated with primary amines at 90 °C for 6 h, the GIC expands to a few layers. The expansion is further facilitated, as the alkyl chain of primary amines becomes longer, while tertiary amines cannot penetrate inside the GIC because of their structural steric hindrance. The primary amine adsorbed in the GIC is oriented to form a bilayer by an indirect reactions among $FeCl_3$–graphene–amine, and this process plays an important role in the expansion of the GIC, in contrast to the reaction of primary amines with donor-type GICs. Then the expanded-GIC is sonicated to exfoliate the graphene sheets. The obtained material exhibited a superparamagnetic property due to the remaining iron compounds. This approach using $FeCl_3$–GIC and primary amine is preferable for the mass production of graphene because of the mild reaction conditions and the short treatment time for exfoliation from the chemically stable $FeCl_3$–GIC. Moreover, the magnetization of graphene nano-composites could be useful for magnetic-recovery processes, electromagnetic heating, and the other applications.

Received 13th October 2013
Accepted 13th December 2013

DOI: 10.1039/c3ta14117a

www.rsc.org/MaterialsA

1. Introduction

Since the first report of its isolation in 2004,[1] graphene has attracted enormous attention in many fields of science because of its astonishing electronic,[2,3] optical,[4] thermal[5] and mechanical properties.[6] As its potential applications expand, the massive synthesis of graphene should be focused on.[7] Although the chemical vapor deposition methods are preferable in terms of the quality of obtained graphene,[8] their synthesis rates are limited. Thus, the mass production of graphene from graphite has been proposed. However, the exfoliation of graphene from graphite by mechanical processes is of low yield, despite many researches using various organic solvents[9–12] and surfactants.[13,14] Supercritical fluids can effectively expand graphite at high pressure;[15] however, it still takes a long time. Then, a chemical modification is required before the exfoliation process. Historically, a monolayer of graphene oxide (GO) was synthesized by Hummer's method, and its modified versions of this method have been reported.[16–18] These methods are based on the intercalation of strong Brønsted acid and the successive penetration of oxidizers. Thus, by the reduction of GO, many defects remain in the obtained graphene due to its functionalization.[19] The defects in graphene sheet adversely affect the unique properties of graphene,[20] and other approaches causing no degradation of the graphene structure are required.

A known approach with a milder oxidation process is the use of a mixture of H_2SO_4 and H_2O_2 to synthesize thermally expandable graphite. In this system, the H_2O_2 molecule generates a gas following pyrolysis at high temperature, and the rapid gas expansion exfoliates the graphite to few-layered graphene.[21] However, the expanded graphite still suffers from oxidation on some level. The utilization of a catalyst can enable the gas expansion exfoliation at low temperature.[22] $FeCl_3$ can be used as a catalyst as well as an intercalator, to facilitate this improvement. The $FeCl_3$ catalyst in graphite can also decompose the hydrazine to generate gas for expansion of the layered structures.[23] Thus, the intercalation into the graphite is the key to opening its layered structure.

Graphite intercalation compounds (GICs) can be obtained by reactions between graphite and various materials.[24–29] The GICs with alkali-metals are available in battery reactions and have been widely investigated. The alkali-metal–GICs are used to make exfoliated graphite.[30–34] The exfoliation mechanisms are classified into 2 types; the intercalation-induction[30,31] and the gas expansion.[32–34] In the intercalation-inducing mechanism, the alkali-metals provide their electrons to graphite and induce the further intercalation of larger molecules to cleave the

[a]Graduate Institute of Applied Science and Technology, National Taiwan University of Science and Technology, 43 Section 4, Keelung Road, Taipei 10607, Taiwan. E-mail: masaki.ujihara@mail.ntust.edu.tw

[b]Department of Chemical Engineering, National Taiwan University of Science and Technology, 43 Section 4, Keelung Road, Taipei 10607, Taiwan. E-mail: imae@mail.ntust.edu.tw

[c]World Premier International Research Center for Materials Nanoarchitectonics, National Institute for Materials Science, 1-1 Namiki, Tsukuba, Ibaraki, 305-0044 Japan

† Electronic supplementary information (ESI) available. See DOI: 10.1039/c3ta14117a

graphite layers. This process can enable the mild exfoliation of graphite without undesired reactions.

In this study, we focused on $FeCl_3$–GIC as the starting material for the intercalation-inducing exfoliation of graphite.[35–37] $FeCl_3$ is a strong Lewis acid and forms a stable acceptor-type GIC. Because the $FeCl_3$–GIC is expected to induce the intercalation of basic materials, several alkyl amines were examined as the secondary intercalator. The structural dependency of the secondary intercalation is discussed. This discussion is helpful to compare the behavior of acceptor-type GICs with the donor-type GICs, and the new approach to exfoliate graphite encourages the mass production of high-quality graphene.

2. Experiments

2.1. Reagents

Triethylamine (TEA) and trihexylamine (THA) were obtained from Alfa Aesar. Hexylamine (HA), dodecylamine (DA), tridodecylamine (TDA), HCl (36.5 wt%), ethanol, and pyridine were purchased from Acros Organics. These materials were in reagent grade and used as supplied. Flake graphites (Z+80: 250–300 μm and Z-5F: 4 μm) were provided from Ito graphite Co., Ltd. Anhydrous iron chloride ($FeCl_3$) was purchased from Acros Organics and dried under vacuum overnight before use.

2.2. Instruments

Raman scattering was measured with a Horiba Jobin Yvon iHR550 imaging spectrometer of with a laser excitation of 633 nm and a laser power of 10 mW. After the specimen was focused at 50-fold magnification on the microscope, the Raman spectrum was recorded at an exposure time of 80 s and an accumulation of 8 scans. Scanning electron microscope (SEM) images were obtained with a JEOL JSM-6500F microscope. X-ray diffraction (XRD) measurement were performed with a Bruker D2 Phaser with CuKα radiation ($\lambda = 0.154$ nm). The small angle X-ray scattering (SAXS) patterns of the obtained samples were characterized by Nano Viewer (RIGAKU, Japan) equipped with a Micro Max-007HF high-intensity microfocus rotating anode X-ray generator with a CuKα radiation source ($\lambda = 0.154$ nm) operating at 40 kV. Thermogravimetric analysis (TGA) was carried out with a Q 500 TA instrument. The specimen was heated from the ambient temperature to 1000 °C at 10.0 °C min^{-1} under air. Atomic force microsope (AFM) measurement was carried out using a Dimension FastScan AFM (Bruker) in the peak force quantitative nanomechanical (QNM) property mapping mode under atmosphere. The dispersion of material was spread on a freshly cleaved mica and dried in air. Magnetization measurement was performed using TM-VSM151483N7-MRO (Tamakawa co.) at ambient temperature.

Treatment of GIC. $FeCl_3$–GIC was synthesized by heating a mixture of graphite and $FeCl_3$. Typically, $FeCl_3$ (10 g) was dried under vacuum at room temperature overnight and was mixed with graphite (2 g) in a glass flask (100 mL). The flask was equipped with a condenser and heated at 337 °C in a muffle furnace for 3 days. Then, the reaction product was cooled down to ambient temperature. The obtained material was a black powder and was used for further experiments.

To expand the obtained GIC, the $FeCl_3$–GIC (0.1 g) was dispersed in an amine (4 mL) and heated at 90 °C for 6 h. Then, the reaction product was filtered, and the residue was washed 10 times with HCl/ethanol (100 mM HCl, 200 mL in total) and once with ethanol (25 mL). The obtained material was dried at 60 °C. For the exfoliation, the dried material (15 mg) was dispersed in pyridine (50 mL), sonicated at room temperature at 50 W for 60 min, and washed by mild centrifugation. This procedure was repeated, and the thus-purified sample was used for AFM measurements.

3. Results and discussion

For the exfoliation of graphene sheets from graphite, intercalation reactions have been applied for pretreatments of graphite; H_2SO_4 and alkali-metals are respectively used to facilitate the further intercalation of oxidizers[16–18,21,27] and other small molecules.[30,31,38] In this study, it was expected that the strong Lewis acid intercalated inside the graphite could induce further penetration of basic materials by acid–base interactions. The intercalation reaction of Lewis acids into graphite is known for various metal halides,[28] and $FeCl_3$–GIC was selected as a typical example of this phenomenon.[35–37] For further intercalation, because of the variety of their molecular structures, primary and tertiary amines with different alkyl chains were used in this study.

The products were characterized by Raman spectroscopy (Fig. 1), and the synthesized $FeCl_3$–GIC was identified as stage-1, because the G-band shifted to 1625 cm^{-1} from 1581 cm^{-1} of the pristine graphite.[36] The large shift in the G-band wavenumber is due to the charge transfer from graphite (donor) to $FeCl_3$ (acceptor), which lowers the Fermi energy level.[39] After the treatment with tertiary amines (TEA, THA and TDA), the G-bands in the products did not change significantly. This suggests that the tertiary amines could not penetrate into the GIC, because of their strong steric hindrance, even if the alkyl chain was short as TEA.

On the other hand, the G-band mostly shifted back to 1580 cm^{-1} after the treatment with primary amines (HA and DA). This indicates that the charge transfer between the graphite and $FeCl_3$ was broken, because the primary amine molecule provided its lone-pair of electrons to $FeCl_3$ to form a complex ($FeCl_3$–amine). The product from HA remained a weak band at 1606 cm^{-1}, which indicated the stage-2 $FeCl_3$–GIC[40] (see ESI, Fig. s1†). The integrated intensity ratio of the G-band against the 2D-band (~2700 cm^{-1}) (Fig. 1) was 0.83 and 0.77 for the HA and DA systems, respectively, while that of the original graphite was 1.11. The low G/2D ratios suggested that these products were graphene with a few layers, and that the product treated by HA was thicker than the DA-treated product.[41] It should be noted that the D-band (~1340 cm^{-1}) was not observed through these processes. That is to say that this process did not degrade the sp^2 lattice structure in graphite.

The morphologies of the products were observed by SEM (Fig. 2). The product treated with DA displayed significantly

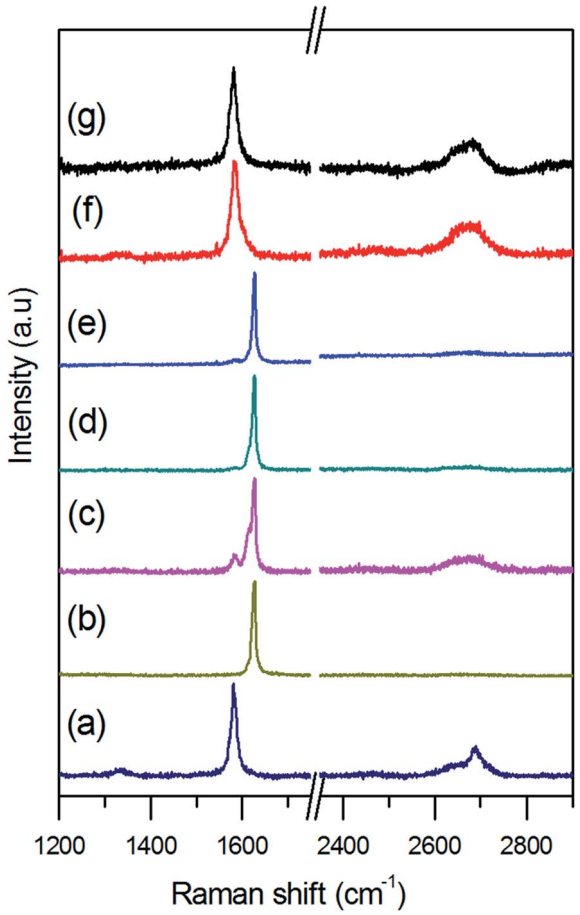

Fig. 1 Raman spectra of (a) graphite, (b) $FeCl_3$–GIC, and $FeCl_3$–GIC after treatment with (c) TEA, (d) THA, (e) TDA, (f) HA, and (g) DA.

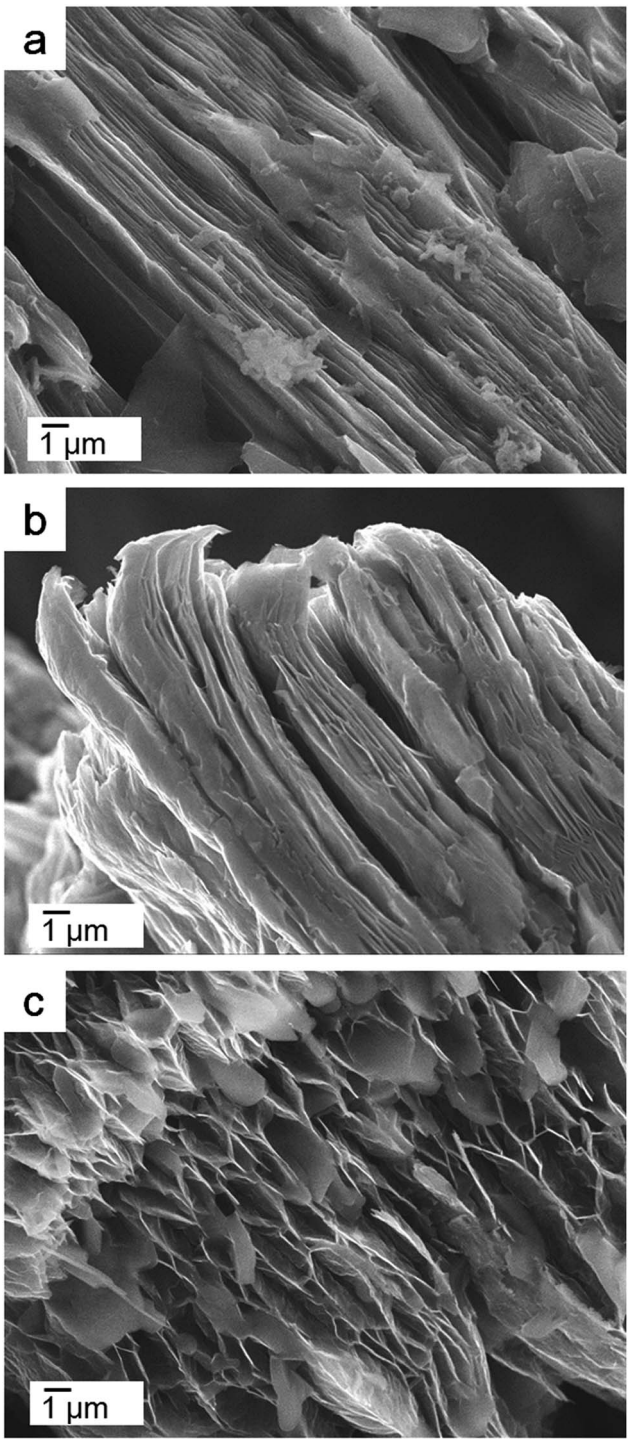

Fig. 2 SEM images of (a) $FeCl_3$–GIC, and $FeCl_3$–GIC after treated with (b) HA, and (c) DA.

expanded layers, and the product treated with HA consisted of less ordered layers. The expanded GIC took on a pie layer-like texture with ultrathin layer units (Fig. 2c). Such a texture was not observed for the other products, which showed only tightly layered structures.

The difference in the layer expansion of GIC was also observed in the XRD results (Fig. 3A). The $FeCl_3$–GIC had a thicker interlayer spacing than the graphite, as can be seen by comparing Fig. 3A(a) and A(b), and its spacing (0.92 nm) corresponded to the stage-1 $FeCl_3$–GIC.[42] The treatment with tertiary amines did not change the XRD pattern of GIC (Fig. 3A(c)–A(e)), which is consistent with the estimation from the Raman scattering and SEM images. Contrastingly, after the treatment with DA and HA, the XRD pattern almost disappeared (Fig. 3A(f) and A(g)). This indicates that the periodical structure of GIC was disturbed by both primary amines.

In order to further prove the penetration of alkyl amines, TGA measurements were carried out (Fig. 4). While the graphite totally decomposed at around 800–1000 °C, $FeCl_3$–GIC resulted in the residue of 40 wt% due to the presence of iron compounds above 870 °C.

The products treated with tertiary amines presented similar behavior to that of $FeCl_3$–GIC. That is, the tertiary amines could not penetrate into the GIC, and therefore $FeCl_3$ was not released by tertiary amines. This is in contrast with the behavior of donor-type GICs, such as alkali-metal GICs, which allow even the penetration of molecules with strong steric hindrance like quaternary ammonium salts.[31]

The treatment with HA resulted in the residue of 32 wt%, which was significantly lower than in the cases of $FeCl_3$–GIC and tertiary amines but much higher than that in the treatment with DA (20% remained). These results suggest that a significant

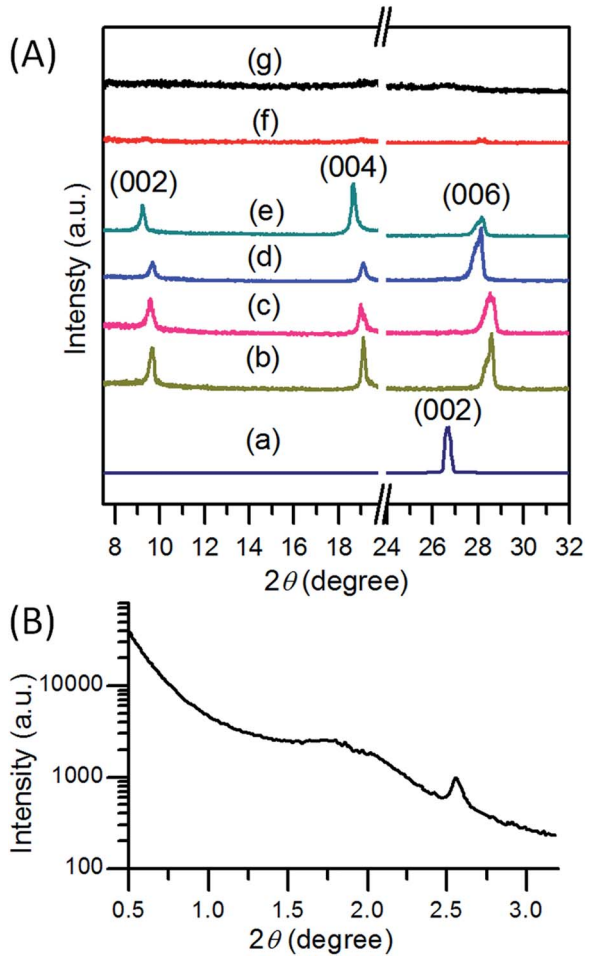

Fig. 3 (A) XRD analyses of (a) graphite, (b) $FeCl_3$–GIC, and $FeCl_3$–GIC after treatment with (c) TEA, (d) THA, (e) TDA, (f) HA, and (g) DA. (B) SAXS analysis of the product after treatment with DA.

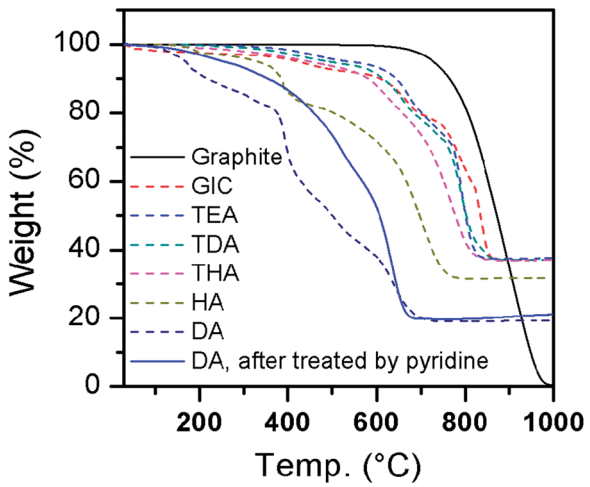

Fig. 4 TGA diagrams of graphite, $FeCl_3$–GIC and $FeCl_3$–GIC after treatment with amines (TEA, THA, TDA, HA, and DA), and DA-treated product after treatment with pyridine.

amount of iron compounds still remains in these products, even after the charge transfer with graphite was broken. On the other hand, the weight loss at around 400 °C could be attributed to the decomposition of amines, which was larger for the DA system than for the HA system. It can be assumed that primary amine molecules are loaded/released in the graphite interlayers, and that the loaded amines bind with $FeCl_3$ in GIC and pull it out on releasing. Long-chain DA can be more abundantly loaded in the graphite interlayers and therefore released more $FeCl_3$ than the short-chain HA. The large extent of encapsulation of DA in $FeCl_3$–GIC and the releasing of $FeCl_3$ coupled with DA from $FeCl_3$–GIC lead the interlayer expansion.

The decomposition temperatures of organic species-loaded $FeCl_3$–GIC were lower than that of $FeCl_3$–GIC; up to 780 °C for HA and up to 700 °C for DA. These lower values also imply the expansion of graphite toward graphene or few-layered graphene, because the decomposition temperature of graphene (~600 °C) is lower than that of $FeCl_3$–GIC.[32,38] These results indicate that the DA molecules expanded the GIC more than the HA molecules did. This may sound strange, because the smaller molecules (HA) could be expected to diffuse into the GIC better than the larger molecules (DA). The high efficiency of DA for the expansion of GIC could be explained by the more hydrophobic character of DA.

The facilitated intercalation of amines with long alkyl chains has also been reported for the donor-type GIC.[38] The Na–GIC swelled by up to 0.7 nm with a single layer of amines with short alkyl chains, however amines with medium length alkyl chains (HA) and long alkyl chains (DA) could form bilayers with a swelled distance of 1.1 nm in the Na–GIC. Meanwhile, the XRD patterns following the reaction process of $FeCl_3$–GIC with DA showed decreasing intensity (Fig. s2†) and did not indicate such repeating distances in its XRD pattern after 6 h treatment (Fig. 3A). However, the SAXS measurements of the product after 6 h treatment with DA indicated the presence of ordered layers separated by 3.46 nm (Fig. 3B and s7†). This distance corresponds to the thickness of graphene (0.34 nm) + the bilayer thickness of DA (chain length of $H_2NC_{12}H_{25}$ = 1.59 nm). This suggests that the $FeCl_3$–GIC interacts with the amine group in DA to orient its alkyl chain perpendicular to the graphene layer in the GIC.

This orientation in $FeCl_3$–GIC is quite different from that in Na–GIC, which allows the bilayer of alkyl amines to lie in a parallel orientation to the graphene layer.[38] This difference can be explained by the interaction of amines with the GICs. In the Na-GIC, the metallic Na donates its electrons to the graphene layer and exists as the cation (Na^+), causing the graphene layer to become electron-rich and therefore negatively charged. The intercalation of amine is driven by the acid–base interaction, and the amine molecules adsorb onto the Na^+ but not to the graphene layer in the GIC.

In contrast, the graphene layer in the $FeCl_3$–GIC is electron-poor because the $FeCl_3$ accepts electrons from graphene.[35] The Fe^{3+} is surrounded by four Cl^- in polymeric $FeCl_3$, which is then sandwiched between the graphene layers,[24,36] thus the amine molecule cannot directly interact with the cation. The lone pair of electrons on the amine should then be attracted to the

electron deficient graphene layer in the $FeCl_3$–GIC. Thus, an indirect acid–base interaction of $FeCl_3$–graphene–amine results in the perpendicular orientation of alkyl amine molecules and their bilayer formation. This bilayer formation should significantly diminish the π–π interaction between the graphene layers, because the effective range of π–π interaction is ~0.8 nm.[43] After loosening the layered structure of GIC, the alkyl amine molecules can directly react with $FeCl_3$, as demonstrated by the Raman results. The broad distances of 4–6 nm suggest the occurrence of aggregates of $FeCl_3$–amine salt between the graphite layers. These aggregates should behave as carriers of $FeCl_3$, transporting it outside of the GIC, or they could be hydrolyzed and precipitated as iron compounds in the following processes. As a control experiment, the graphite was subjected to a mixture of $FeCl_3$ with DA at 90 °C. The graphite was not exfoliated in this process. Thus, the observed expansion of $FeCl_3$–GIC with DA was not due to solubilization by the $FeCl_3$–amine salt, demonstrating that the two-step intercalation of $FeCl_3$ and amine is essential for the exfoliation in this method.

In contrast to the synthesis of graphene oxide,[16–20,44,45] the present reaction is not destructive with respect to the graphene structure. The ultrathin layers of expanded graphite were partially connected to each other like pie layers (Fig. 2c), and then the treatment with DA could not remove all of the $FeCl_3$ in the $FeCl_3$–GIC (Fig. 4). Even when the reaction was carried out at higher temperature (250 °C) or using an amine with a longer alkyl chain (octadecylamine), the ratio of residual $FeCl_3$ was not significantly decreased (see Fig. s3†).

Then, further purification was performed by sonication in pyridine to exfoliate the layers mechanically. After sonication for 60 min, the remaining DA was removed as shown by the subsequent lack of weight loss at ~400 °C; however, residual impurities still remained at 20 wt% above 680 °C (Fig. 4). The residual impurities were considered to be iron oxides, such as Fe_3O_4 or γ-Fe_2O_3 (Fig. s4†), which were formed *via* decomposition of the $FeCl_3$–amine salt with moisture in ethanol during the washing process.[46] To remove the iron oxides from the product, strong acid treatment was carried out; however, the residual impurities were found to be durable even under the strong acid conditions (Fig. s5†).

The removal of small molecules (DA) and the remaining iron compounds suggest that the iron compounds deposited on graphene. In a transmission electron microscope observation (Fig. s6†), the remaining iron compounds appeared as black domains with a size of several nm. To confirm the structure of the product, AFM analysis was performed for the specimen sonicated in pyridine (Fig. 5). A film-like texture was observed and its thickness was 1–2 nm, which was consistent with single or few-layered graphene with iron oxides, as expected from the Raman spectroscopy and TGA analyses mentioned above.

Thus, it was suggested that there were three steps in the expansion of $FeCl_3$–GIC: (1) the penetration of alkyl amine molecules into the GIC, (2) the bilayer formation of the adsorbed alkyl amine molecules between the graphene layers, and (3) the removal and precipitation of iron compounds (Scheme 1). The product was considered the nano-composite of few-layered graphene with iron-oxide.

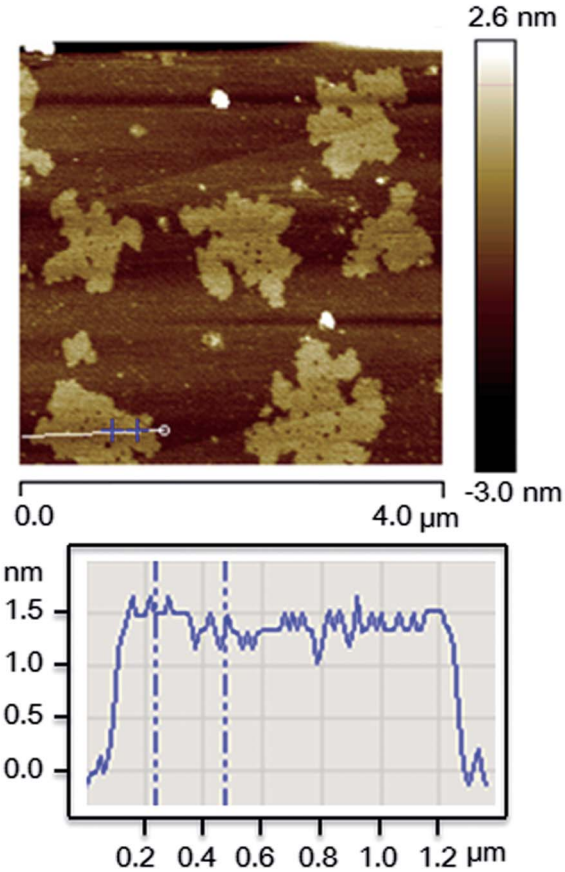

Fig. 5 AFM image and cross-sectional analysis of graphene prepared from $FeCl_3$–GIC by DA treatment and sonication in pyridine.

To characterize this nano-composite, the magnetization of the DA/pyridine-treated product was measured (Fig. 6). While the graphite and $FeCl_3$–GIC had weak paramagnetism, the DA/pyridine-treated product exhibited superparamagnetism, as typically do the nanostructures of magnetic iron oxides.[46,47] Thus, the obtained material can be used as a magnetic nano-composite with excellent durability, and the easy synthesis would be suitable for practical applications.

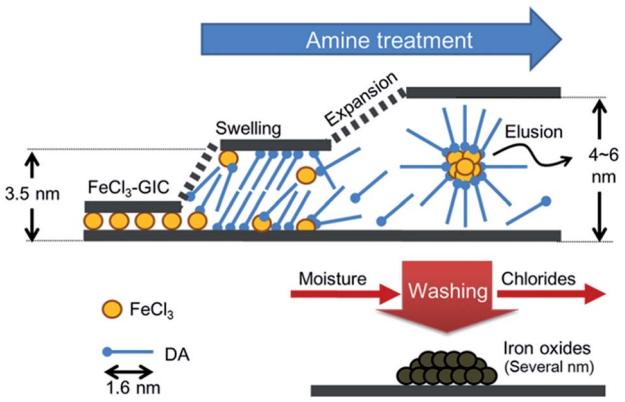

Scheme 1 Expansion process of $FeCl_3$–GIC by amine treatment and formation of iron-oxide domains.

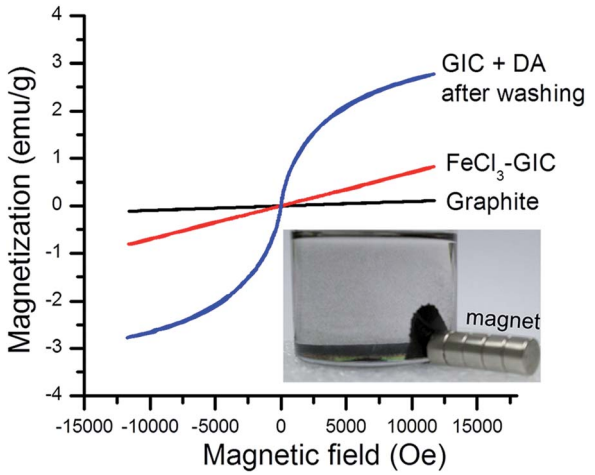

Fig. 6 Magnetization of the graphite, $FeCl_3$–GIC, and the DA-treated GIC after sonication with pyridine. Inset: photograph of the DA-treated GIC dispersed in pyridine after sonication.

4. Conclusions

Graphene was obtained by the reaction of $FeCl_3$–GIC of stage-1 with primary amines. When the reaction was carried out at 90 °C for 6 h, the product was the expanded graphite with pie-like structure of ultrathin layers. This behavior was explained by the bilayer formation of the alkyl amine molecules. In this process, an indirect interaction between $FeCl_3$–graphene–amine was suggested to play an important role. The amine with longer alkyl chains (C_{12}) expanded the GIC more effectively than the amine with shorter chains (C_6) and, meanwhile, tertiary amines could not penetrate inside the GIC because of their strong steric hindrance. The mechanism is in contrast with the expansion of donor-type GICs and will be useful for the further understanding of graphite expansion.

The TGA analysis indicated that a significant amount of iron compounds remained in the expanded graphite due to the imperfect destruction of the interlayer interaction in this process, even after sonication in pyridine. AFM analysis confirmed that the product consisted of ultrathin films of 1–2 nm in thickness, and the magnetization of the product indicated the superparamagnetic property as is the typical behavior of such nanostructures of iron oxides. This method is applicable for the mass-production of graphene with magnetic properties, because the starting material ($FeCl_3$–GIC) is chemically stable, the reaction conditions are mild and the reaction time is short. The excellent durability of this nano-compound can be used to facilitate magnetic-recovery processes, electromagnetic heating, and the other applications in drastic conditions.

References

1 K. S. Novoselov, A. K. Geim, S. V. Morozov, D. Jiang, Y. Zhang, S. V. Dubonos, I. V. Grigorieva and A. A. Firsov, *Science*, 2004, **306**, 666–669.
2 A. K. Geim and K. S. Novoselov, *Nat. Mater.*, 2007, **6**, 183–191.
3 R. M. Westervelt, *Science*, 2008, **320**, 324–325.
4 A. B. Kuzmenko, E. van Heumen, F. Carbone and D. van der Marel, *Phys. Rev. Lett.*, 2008, **100**, 117401, DOI: 10.1103/PhysRevLett.100.117401.
5 A. A. Balandin, S. Ghosh, W. Bao, I. Calizo, D. Teweldebrhan, F. Miao and C. N. Lau, *Nano Lett.*, 2008, **8**, 902–907.
6 A. K. Geim and K. S. Novoselov, *Nat. Mater.*, 2007, **6**, 183.
7 M. Segal, *Nat. Nanotechnol.*, 2009, **4**, 612–614.
8 X. S. Li, W. W. Cai, J. H. An, S. Kim, J. Nah, D. X. Yang, R. Piner, A. Velamakanni, I. Jung, E. Tutuc, S. K. Banerjee, L. Colombo and R. S. Ruoff, *Science*, 2009, **324**, 1312–1314.
9 Y. Hernandez, V. Nicolosi, M. Lotya, F. M. Blighe, Z. Y. Sun, S. De, I. T. McGovern, B. Holland, M. Byrne, Y. K. Gun'ko, J. J. Boland, P. Niraj, G. Duesberg, S. Krishnamurthy, R. Goodhue, J. Hutchison, V. Scardaci, A. C. Ferrari and J. N. Coleman, *Nat. Nanotechnol.*, 2008, **3**, 563–568.
10 J. N. Coleman, *Adv. Funct. Mater.*, 2009, **19**, 3680–3695.
11 U. Khan, A. O'Neill, M. Lotya, S. De and J. N. Coleman, *Small*, 2010, **6**, 864–871.
12 Z. Tang, J. Zhuang and X. Wang, *Langmuir*, 2010, **26**, 9045–9049.
13 S. Vadukumpully, J. Paul and S. Valiyaveettil, *Carbon*, 2009, **47**, 3288–3294.
14 S. M. Notley, *Langmuir*, 2012, **28**, 14110–14113.
15 L. Li, X. Zheng, J. Wang, Q. Sun and Q. Xu, *ACS Sustainable Chem. Eng.*, 2012, **1**, 144–151.
16 W. S. Hummers and R. E. Offeman, *J. Am. Chem. Soc.*, 1958, **80**, 1339.
17 N. I. Kovtyukhova, P. J. Ollivier, B. R. Martin, T. E. Mallouk, S. A. Chizhik, E. V. Buzaneva and A. D. Gorchinskiy, *Chem. Mater.*, 1999, **11**, 771–778.
18 D. C. Marcano, D. V. Kosynkin, J. M. Berlin, A. Sinitskii, Z. Sun, A. Slesarev, L. B. Alemany, W. Lu and J. M. Tour, *ACS Nano*, 2010, **4**, 4806–4814.
19 K. N. Kudin, B. Ozbas, H. C. Schniepp, R. K. Prud'homme, I. A. Aksay and R. Car, *Nano Lett.*, 2007, **8**, 36–41.
20 L. Tang, Y. Wang, Y. Li, H. Feng, J. Lu and J. Li, *Adv. Funct. Mater.*, 2009, **19**, 2782–2789.
21 W. Gu, W. Zhang, X. Li, H. Zhu, J. Wei, Z. Li, Q. Shu, C. Wang, K. Wang, W. Shen, F. Kang and D. Wu, *J. Mater. Chem.*, 2009, **19**, 3367–3369.
22 X. M. Geng, Y. F. Guo, D. F. Li, W. W. Li, C. Zhu, X. F. Wei, M. L. Chen, S. Gao, S. Q. Qiu, Y. P. Gong, L. Q. Wu, M. S. Long, M. T. Sun, G. B. Pan and L. W. Liu, *Sci. Rep.*, 2013, **3**, 1134, DOI: 10.1038/srep01134.
23 A. Messaoudi, M. Inagaki and F. Beguin, *Mater. Sci. Forum*, 1992, **91–93**, 811–816.
24 M. S. Dresselhaus and G. Dresselhaus, *Adv. Phys.*, 2002, **51**, 1–186.
25 N. Akuzawa, J. Yoshioka, C. Ozaki, M. Tokuda, K. Ohkura and Y. Soneda, *Mol. Cryst. Liq. Cryst.*, 2002, **388**, 415–421.
26 H. Shioyama, M. B. H. M. Saman and A. J. Sanpanich, *J. Mater. Res.*, 2002, **17**, 3190–3192.
27 K. H. Park, B. H. Kim, S. H. Song, J. Kwon, B. S. Kong, K. Kang and S. Jeon, *Nano Lett.*, 2012, **12**, 2871–2876.
28 A. M. Dimiev, S. M. Bachilo, R. Saito and J. M. Tour, *ACS Nano*, 2012, **6**, 7842–7849.

29 K. C. Kwon, K. S. Choi and S. Y. Kim, *Adv. Funct. Mater.*, 2012, **22**, 4724–4731.
30 J. M. Englert, C. Dotzer, G. Yang, M. Schmid, C. Papp, J. M. Gottfried, H. P. Steinrück, E. Spiecker, F. Hauke and A. Hirsch, *Nat. Chem.*, 2011, **3**, 279–286.
31 W. Sirisaksoontorn, A. A. Adenuga, V. T. Remcho and M. M. Lerner, *J. Am. Chem. Soc.*, 2011, **133**, 12436–12438.
32 L. M. Viculis, J. J. Mack, O. M. Mayer, H. T. Hahn and R. B. Kaner, *J. Mater. Chem.*, 2005, **15**, 974–978.
33 J. Kwon, S. H. Lee, K. H. Park, D. H. Seo, J. Lee, B. S. Kong, K. Kang and S. Jeon, *Small*, 2011, **7**, 864–868.
34 H. Huang, Y. Xia, X. Tao, J. Du, J. Fang, Y. Gan and W. J. Zhang, *J. Mater. Chem.*, 2012, **22**, 10452–10456.
35 D. Zhan, L. Sun, Z. H. Ni, L. Liu, X. F. Fan, Y. Wang, T. Yu, Y. M. Lam, W. Huang and Z. X. Shen, *Adv. Funct. Mater.*, 2010, **20**, 3504–3509.
36 W. Zhao, P. H. Tan, J. Liu and A. C. Ferrari, *J. Am. Chem. Soc.*, 2011, **133**, 5941–5946.
37 I. Khrapach, F. Withers, T. H. Bointon, D. K. Polyushkin, W. L. Barnes, S. Russo and M. F. Craciun, *Adv. Mater.*, 2012, **24**, 2844–2849.
38 T. Maluangnont, G. T. Bui, B. A. Huntington and M. M. Lerner, *Chem. Mater.*, 2011, **23**, 1091–1095.
39 A. Jorio, M. S. Dresselhaus, R. Saito and G. Dresselhaus, *Raman Spectroscopy in Graphene Related Systems*, Wiley, 2010.
40 T. Abe, Y. Mizutani, M. Asano, T. Harada, M. Kawase, S. Tanaka and M. Kamada, *Carbon*, 1996, **34**, 1160–1161.
41 D. Graf, F. Molitor, K. Ensslin, C. Stampfer, A. Jungen, C. Hierold and L. Wirtz, *Nano Lett.*, 2007, **7**, 238–242.
42 D. Begin, E. Alain, G. Furdin and J. F. Mareche, *J. Phys. Chem. Solids*, 1996, **57**, 849–854.
43 M. Jin, H. K. Jeong, T. H. Kim, K. P. So, Y. Cui, W. J. Yu, E. J. Ra and Y. H. Lee, *J. Phys. D: Appl. Phys.*, 2010, **43**, 275402.
44 B. Shen, D. Lu, W. Zhai and W. Zheng, *J. Mater. Chem. C*, 2013, **1**, 50–53.
45 M. Jin, T. H. Kim, S. C. Lim, D. L. Duong, H. J. Shin, Y. W. Jo, H. K. Jeong, J. Chang, S. Xie and Y. H. Lee, *Adv. Funct. Mater.*, 2011, **21**, 3496–3501.
46 S. Thimmaiah, M. Rajamathi, N. Singh, P. Bera, F. Meldrum, N. Chandrasekhar and R. Seshadri, *J. Mater. Chem.*, 2001, **11**, 3215–3221.
47 W. Zhang, X. Shi, Y. Zhang, W. Gu, B. Li and Y. Xian, *J. Mater. Chem. A*, 2013, **1**, 1745–1753.

